

UNDERGROUND OBJECT DETECTION BASED ON RADIO PROPAGATION CHARACTERISTICS

SUHERMAN^{1*}, ERWIN WIJAYANTO¹, ALI HANAFIAH RAMBE¹, NAEMAH MUBARAKAH¹, YULIANTA SIREGAR¹, MARWAN AL-AKAIDI²

¹Electrical Engineering Department, Universitas Sumatera Utara, Medan, Indonesia

²American University in the Emirates, Dubai, UAE

E-mail: *suherman@usu.ac.id

ABSTRACT

Underground object detection is useful to explore underground resources as well as to monitor underground infrastructure. Underground object detection has been employed for mineral exploration, archeological material finding and underground fault detection. Existing systems usually employ the ground penetration radar (GPR) that makes use radio signal reflection. GPR weakness is that the device relies only on a single point of signal receptions that minimize the scope of detection. This paper proposes multipoint radio receptions for underground object detection based on the received signals instead of the reflected ones. The proposed system was initially tested experimentally for bandwidth range of 97 MHz to 130 MHz which results error shifting from the employed model about 50.33% at frequency 130.762 MHz, 17.58% at 109.818 MHz and 13.38% at 97.335 MHz. Method of finding the best frequency is then developed by employing gradient comparison. Higher frequencies were chosen from 500 MHz to 1 GHz as these frequency results worse losses to ensure experiments were conducted in the worst condition. The analysis found that 537.69 MHz is the best frequency for the frequency range. In order to reconstruct the detected object, the number of multipath propagations is then determined. The object detections were then measured based on the supervised and unsupervised techniques. The supervised method exerted better precision compared to the unsupervised method by at least 30% with the detected object reducing the received signal up to 1.86 dBm or 2.68% in average.

Keywords: *Underground object detection, radio propagation losses, propagation model*

1. INTRODUCTION

Signal propagation experiences losses in transmission media due to the nature of signal propagation. Signal loss worsen when it propagates in soil and water [1]. The attenuation is in form of decrement on signal amplitude and shifting in signal phase. Signal decrement and shifting are caused by media dispersion, signal absorption, and signal scattering [2]. The underground structure that comprises soil with different characteristics, water and mineral mixture makes it difficult to predict the propagation characteristics. Changes on transmission parameter result significant error shifting. This reason underpins the use of reflected signal to determine underground object in ground penetration radar (GPR) technologies. Although the alternative technologies, such as electromagnetic induction [3], time domain reflectometer and capacitance measurement [4, 5] are exist, but the application is limited.

The very high frequency band (VHF) is preferred when deal with underground signal

propagation like into the earth (TTE) radio for mining industry [6]. This band is safe enough for high power radiation and less sensitive to ground absorption than the higher spectrum.

Beside for object detection, the application of underground radio, TTE has been used since long time ago, mainly for supporting audio and data communication in mining industries [7], including the operation of underground wireless sensor networks (WSNs) for detecting particular events, locating the miners and preventing the construction failures [1]. The stability of the underground structure should be monitored as rock mass surrounding the construction is crucial for underground safety [2]. TTE including GPR are also used for near surface construction detection such as buried pipeline and also to measure surface depression impact [3].

Underground natural phenomenon such as water impoundment, fluid subsurface, gasses and hydrocarbon extraction, water composition are also employed this technology [7]. Sensitive

underground nuclear experiment also needs this technology [8].

Underground material rapidly reduces radio signal that makes radio signal is difficult to travel long distance. Abdul Salam [9] plotted the power density of electrical field components as in Figure 1 that is rapidly decreasing to transmitter receiver distance. For less than 1 m depth, the horizontal electrical field is rapidly weakened about 11 dB than in vertical direction.

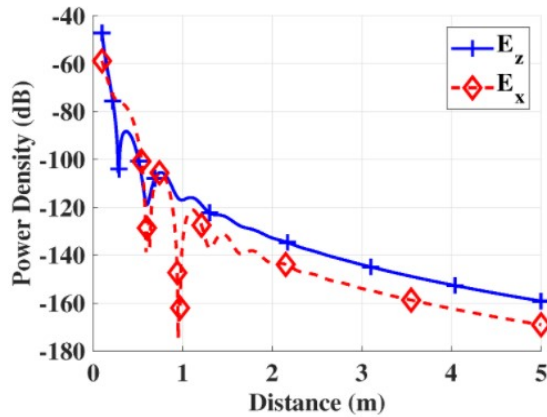


Figure 1. Power density decrement [9]

In order to predict the propagation characteristic, many researchers proposed the transmission model [10, 11]. Wireless underground was initially based on the Friis transmission formula [10], followed by the impulse response and multi-carrier model [12, 13]. The statistical model was developed based on empirical formula and testbed [14]. Analytical model has been research interests such as Sommerfeld integral [15], Zenneck-wave-based UGchannel model [16]. However, analytical was developed based on electromagnetic approximation which is erroneous when antenna defected.

This paper is aimed to analyses the capability of multipoint signal receptions in predicting the underground object that are passed through by the transmitted signals. Experimental approach and channel modeling with low VHF and high VHF frequency bands are applied to assess the object prediction. Paper is organized as follows. Mathematical model based on Friis formula is given in the next section followed by three-dimensional coordinate analysis, and measurement model. Experimental circuit for low VHF frequency generator and the used of vector network analyzer as well as measurement plane are outlined in research method section. Results analysis and conclusion are then followed.

2. MATHEMATICAL MODELS

This paper makes use underground Friis model with corrected parameters, propagation line model, and propagation path mathematical expression

2.1 Underground signal propagation

The Friis transmission formula is named after Harald T. Friis, a Danish-American engineer, that is widely used for predicting the received power at the antenna terminal. The formula multiplied the incident wave power density and the effective aperture of the idealized antenna as in Equation 1.

$$P_r / P_t = A_r A_t / (d^2 \lambda^2) \quad (1)$$

Friis equation to predict propagation lossess considers distance, frequency and ground properties. The received power is calculated based on Equation 2 where losses are lumped into single L_1 parameter [17]:

$$P_r(\text{dBm}) = P_t(\text{dBm}) + G_r(\text{dB}) + G_t(\text{dB}) - L_1(\text{dB}) \quad (2)$$

The lumped loss L_1 comprises free space loss L_0 which is approximated by using distance (d in km) and frequency (f in MHz):

$$L_0(\text{dB}) = 32.4 + 20 \log(d) + 20 \log(f) \quad (3)$$

and ground loss L_s . L_s accommodates signal attenuation, signal scattering and and signal distortion depending upon the parameters of α and β . The parameter α is the attenuation constant measured in 1/m which varies over different soil water mixtures. The parameter β is measured in radian/m as the phase shifting of the signal caused by the media. The value of L_s is approximated as in Equation 4 [17, 18].

$$L_s = 8.69\alpha d + 154 - 20\log(f)(\text{Hz}) + 20\log(\beta) \quad (4)$$

The constant of α and β are determined based on Equation 5 and 6 [4]:

$$\alpha = \omega \sqrt{\frac{\mu \epsilon'}{2} \left[\sqrt{1 + \left(\frac{\epsilon''}{\epsilon'}\right)^2} - 1 \right]} \quad (5)$$

$$\beta = \omega \sqrt{\frac{\mu \epsilon'}{2} \left[\sqrt{1 + \left(\frac{\epsilon''}{\epsilon'}\right)^2} + 1 \right]} \quad (6)$$

Parameter μ is the permeability of the ground, while ϵ' and ϵ'' are the real and imaginary values of the permittivity. Most ground

permeability is assumed as free space: $\mu = \mu_0$ and $\mu_0 = 1$ [19].

$$pos = \left(\frac{l}{s} + 1\right) \cdot n \tag{8}$$

2.2 Propagation line model

The three-dimensional line equation is needed to detect points passed through by the propagated signal so that the exact location of the detected material is known. Mathematical model uses the three-dimensional space described in [20].

The line L is passed through point P(x0, y0, z0) and considered parallel to vector $v = \langle a, b, c \rangle$ only if Q = (x, y, z) makes vector PQ parallel to v. This line PQ is expressed by vector $PQ = \langle x-x_0, y-y_0, z-z_0 \rangle$ so that PQ is parallel to v fulfilling the equation $PQ = t \cdot v$. Parameter t is a scalar. Point x, y, and z are determined by Equation 7. Figure 2 illustrates the line.

$$\langle x, y, z \rangle = \langle x_0 + ta, y_0 + tb, z_0 + tc \rangle \tag{7}$$

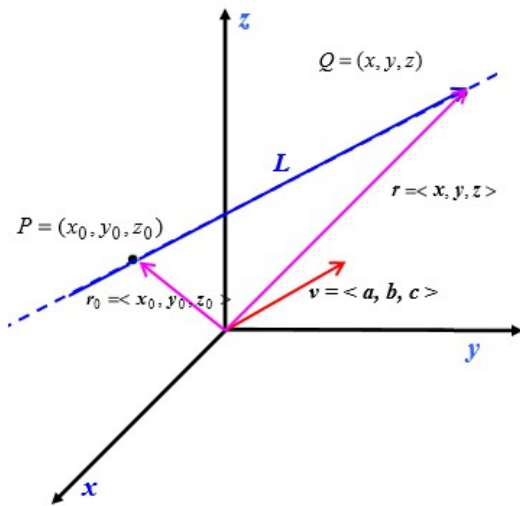


Figure 2. Three-dimensional line model [19]

2.3 Separated transceiver model

In order to measure signal level that is used to enable prediction on the underground object, three-dimensional measurement should be conducted. The three-dimensional room model is proposed to calculate how many positions of transmitter and receiver that are probable to detect the object.

It is assumed that the evaluated underground volume is in form of cubical shape with edge l (Figure 3). The transmitter and receiver are inserted to the ground at n vertical edges with step variations of s. The number of transmitter and receiver position in measurement can be calculated based on Equation 8.

For instance, if the evaluated underground space has edge size of l = 5 m, the vertical edge n=2, and position variation steps s = 1 m, there are 6 transmitter positions and 6 receiver position. Number of propagation path can be calculated as in Equation 9. For this example, number of propagation paths is 36.

$$p = \binom{n}{2} \cdot (l/s + 1)^2 \tag{9}$$

If it is assumed that decreasing received signal denotes underground object blocking and high level of received signal means non blocking path, then the location of transmitter i and receiver j, $p_{i,j}$ can be predicted as blocked or passed through i by using the Equation 10.

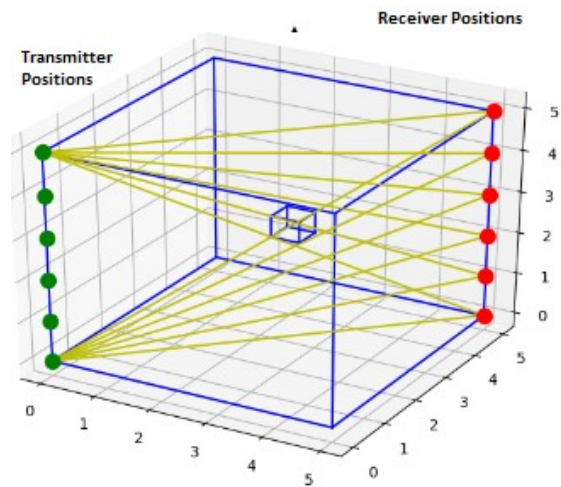


Figure 3. Measurement model

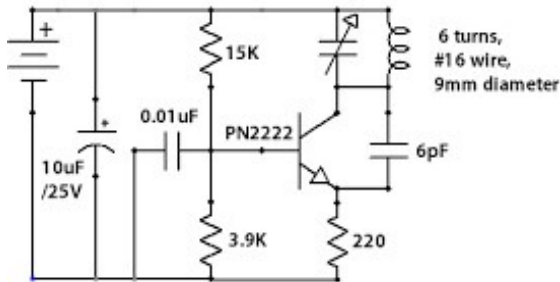
$$p_{i,j} = \begin{cases} \text{Blocked, if } P_r < f \cdot P_{rmax\ i,j} \\ \text{Unblocked, if } > f \cdot P_{rmax\ i,j} \end{cases} \tag{10}$$

3. RESEARCH METHOD

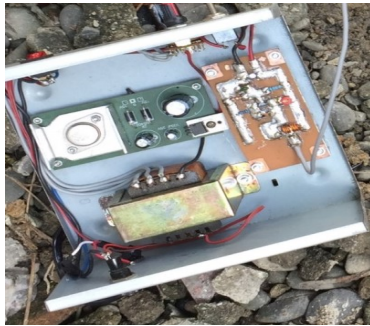
In order to analyses the signal and the object prediction, the experiments are divided into two parts. The first assessment on familiar parts. The first assessment on familiar parts. The frequency band of 97 MHz to 130 MHz is selected. The second assessment on frequency band of 500MHz to 1 GHz is performed as the attenuation and scattering worsen at this band so that system is assessed in the worst condition.

3.1 Low Frequency Assessment

In order to detect the underground object using frequency range of 97 MHz to 130 MHz, a simple frequency modulation transmitter is devised as in Figure 4. The transistor PN2222 is biased by using a voltage divider of 15K and 3.9K with LC tank at the collector. The voltage divider produces sufficient collector voltage to swing and gives sufficient transmitting power. Collector current flows through LC.



(a) Signal generator circuit



(b) Signal generator module

Fig. 4. Low VHF Frequency Signal generator



Fig. 5. Vector network analyzer

The transistor amplifies signal within frequency range of 97 MHz to 130 MHz, so that collector current falls to these frequencies. Oscillated signal is then fed back to input base by using 0.01uF capacitor. The generated frequency is adjusted by using capacitor variable at LC tank. The wire of 6 turns 9 mm is used for coil making. Figure 4b shows the implemented circuit.

A 9 V independent battery is used to activate circuit. However, level can be decreased by adapting voltage source to 6 Volt, 7.5 Volt and 9 Volt. A spectrum analyzer is employed to receive the transmitted signal.

The antenna is devised by using a $1/8 \lambda$ wire monopole antenna for both transmitter and receiver. The signal measurement is plotted by using the scenario as depicted in Figure 6.

The permittivity parameters for the observed land are approximated as in [8] with ϵ' and ϵ'' values are set 6.53 and 1.88 respectively.

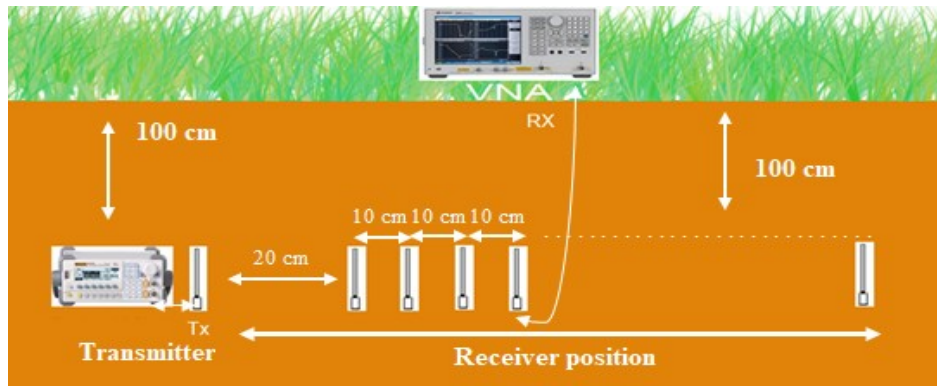


Fig. 6. Measurement plan

3.2 Multipoint Assessment

Multipoint assessment was conducted for frequency of 500 MHz to 1 GHz. The assessments

were divided into: best frequency assessment, unsupervised measurement and supervised measurement.

In order to enable propagation characteristics to reveal underground object, best frequency should be used to fit the ground composition. In order to do so, the following steps were taken.

- Measurements are performed for specific frequency and distance. Received signal levels for different frequency and distance are recorded.
- Simulations are performed for similar frequency and distance.
- Calculated gradients for both experiments and simulations results.
- Negative gradient is preferred as logically signal decreases as distance increases.
- Find the frequency with the lowest gradient differences between experiment and simulation. This frequency is selected for measurement.

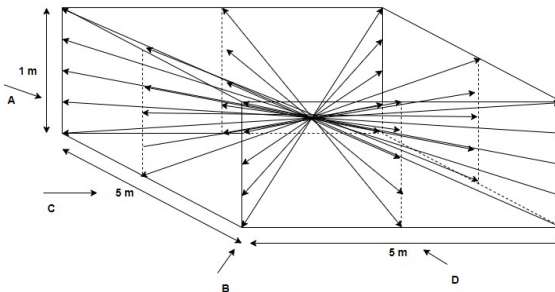
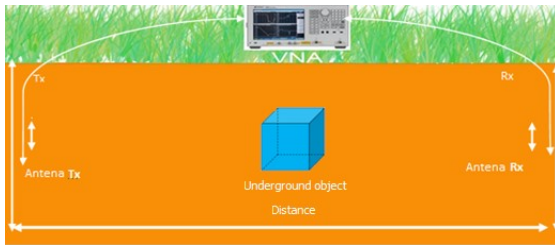


Fig. 7 Vector network analyzer radio paths

Fig. 7 shows the measurement line to detect an object. The object is positioned in the center of the evaluated area. The method is just to show the effectiveness of the system. In order to apply on real object, other method may apply. The underground object is a metal box 8000 cm³. For the evaluated frequency band 500 MHz to 1 GHz, the VNA is used for both transmitter and receiver.

For higher transmitting power and reception sensitivity, another device can be employed. Limited propagation lines are chosen in

this experiment (Figure 7b). More complicated propagation lines are possible if the receiver and transmitter can be shifted automatically.

4. RESULTS AND ANALYSIS

4.1 97 MHz to 130 MHz Measurement Results

The measurement results for frequency band of 97 MHz to 130 MHz are represented by three chosen frequencies 97.335 MHz, 109.818 MHz, and 130.762 MHz. The signal is rapidly attenuated by the ground material as depicted in Figure 8.

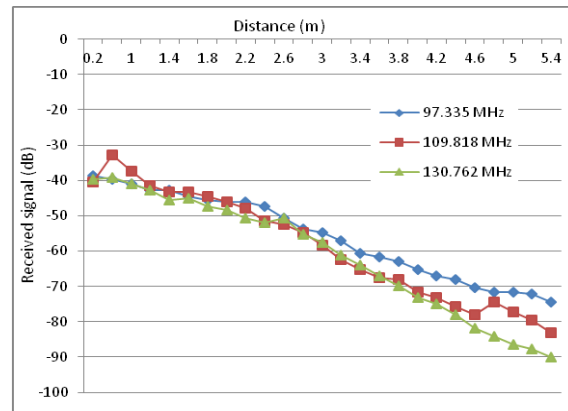


Fig. 8 Signal attenuation

Figure 9, Figure 10 and Figure 11 show the comparisons of the measured signals to the propagation model for frequency 97.335 MHz, 109.818 MHz, and 130.762 MHz as chosen frequencies in 97 MHz to 130 MHz. Both measurement and model results show that signals decrease rapidly due to distance increment.

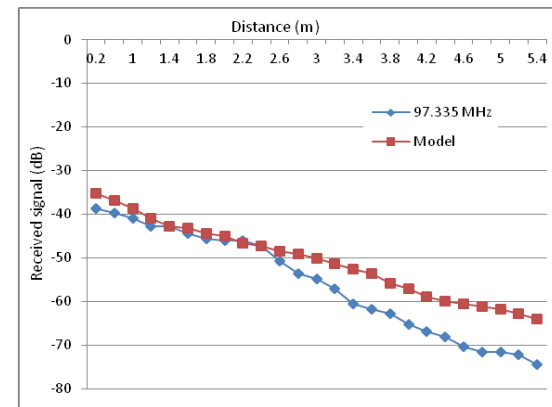


Fig. 9 Received signal vs model for 97.335 MHz

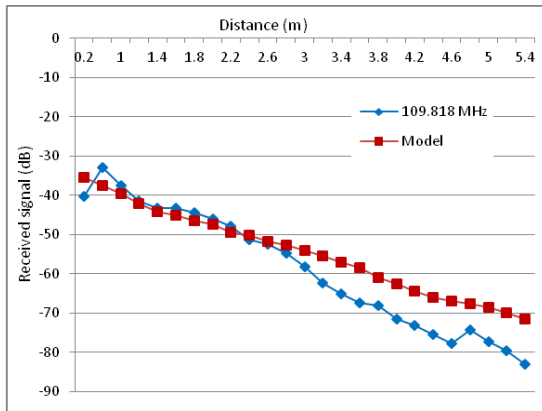


Fig.10 Received signal vs model for 109.818 MHz

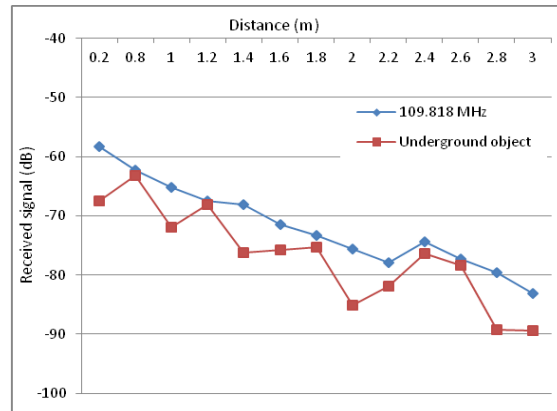


Fig.13 Impact of the underground object for 109.818 MHz

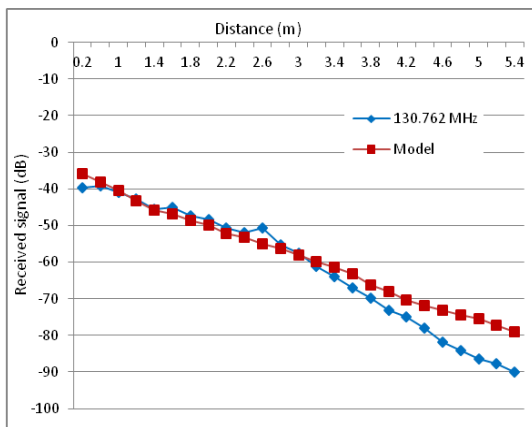


Fig.11 Received signal vs model for 130.762 MHz

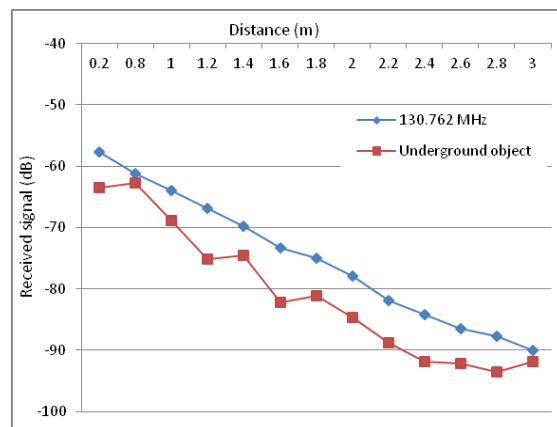


Fig.14 Impact underground object for 130.762 MHz

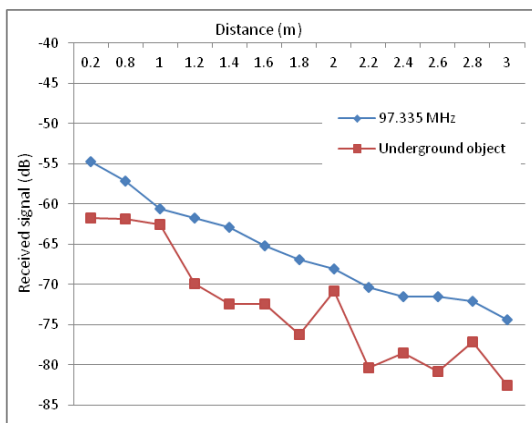


Fig.12 Impact underground object for 97.335 MHz

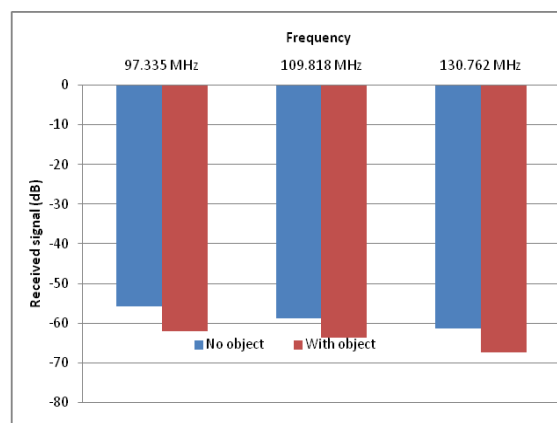


Fig.15 Average signal decrement due object detection

Meanwhile, Figure 12, Figure 13, and Figure 14 show that signal decrement can be distinguished between direct signal or blocked signal due to the existence of the underground object that is inserted in between transmitter and receiver. The average signal decrement is shown in Figure 15.

By comparing the differences between measured signal with the employed model and the no object signal and the detected object signals, it can be determined which frequency has the best performance. Figure 16 show that the frequency of 130.762 MHz has the best precision as it has the smallest average model error. However, frequency of 109.818 MHz has the best capability in detecting object as it has the highest signal decrement.

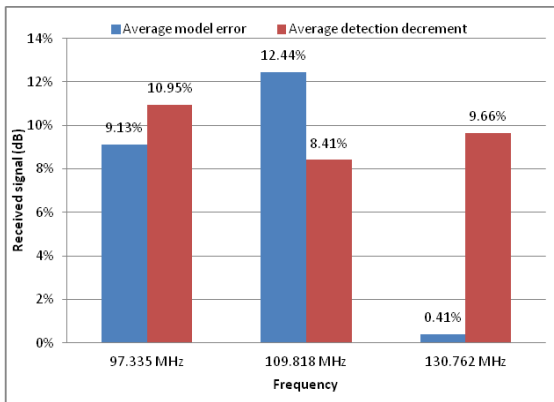


Fig.16 Average signal decrement due object detection

4.2 Multipoint propagation analysis

Figure 17 shows the sample of measurement results for measurement on frequency band of 500 MHz to 1 GHz. At this frequency band, signal varies very rapidly. This variation is influenced by underground scattering characteristic that differs from one frequency to other frequencies.

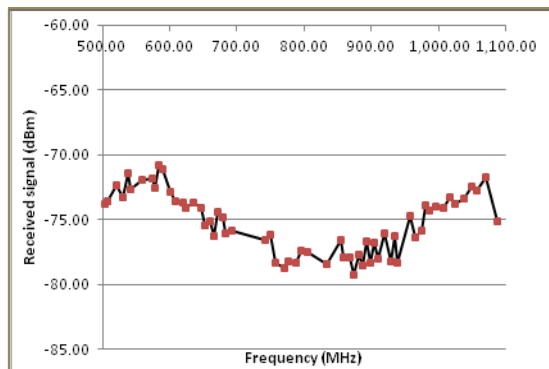


Fig.17 Received signal level for frequency band 500 MHz to 1 GHz

Unlike surface propagation, signal decrease inconsistently to distance (Figure 18). Therefore, it is necessary to find the best frequency for difference underground media. The following technique is suggested to make sure the working frequency is the best one to deal with the type of underground media.

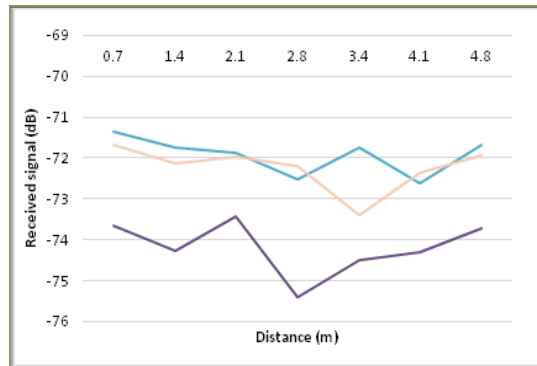


Fig.18 Sample received signal level for various distance

Figure 19 shows the results of the mathematical model for frequency band of 500 MHz to 1 GHz. The higher the frequencies the lower the received signal level. Frequency 500 MHz has the exponential losses while frequency 1 GHz has the most constant attenuation to all transmitter receiver distances. It means the highest frequency has homogenous responses to ground attenuation. However, the signal level is very low.

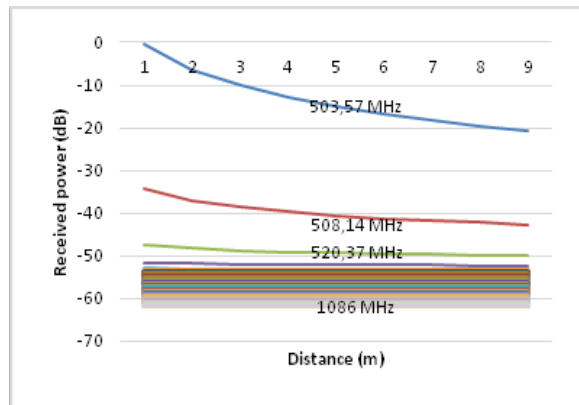


Fig.19 Modeled received signal for frequency band 500 MHz-1 GHz

In order to find best frequency, both measurement and model results are compared by using tangential values. All the tangential values for both measurements and models are plotted in Figure 20.

Selection criteria for the selected frequency are, both measurement and model tangential values should be negative and has the

smallest differences. Tangential values vary for different frequency. Some frequencies have increasing signal pattern due to multipath propagation and signal scattering.

As result, frequency of 537.69 MHz is selected as the best working frequency. Figure 21 shows the level of the received signal for the selected frequency, 537.69 MHz for various distances. This working frequency is used for detecting the underground object by considering two techniques: supervised and unsupervised measurement.

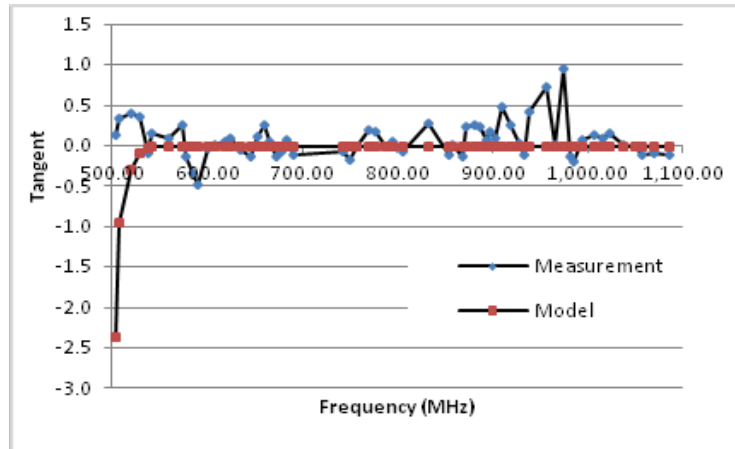


Fig.20 Tangential values

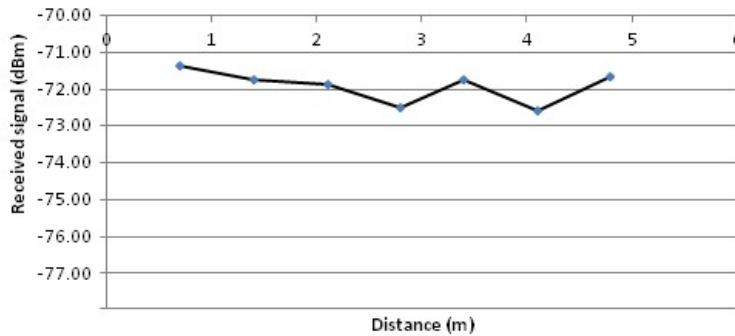


Fig.21 Samples of received signals for the selected frequency

In order to determine the existence of the underground object, two ways are performed. The first way is by using supervised measurement. This method requires that initial condition, the received signal levels before the underground object exist should has been known. This method can be used to monitor land or underground structure changes. This method cannot be used to explore object in unknown environment.

The second method is unsupervised measurement. The unsupervised measurement compares received signal level to predicted model.

A threshold should be developed to ensure either underground object exists or not. The decision of a transmission path is blocked by and objects or not is determined by the following code snippet.

```

for (i=0; i<number_of_position; i++)
    for (j=0;j<number_of_position)
        if (i!=j){
            MaxReceivedPower(i,j)=PropagationModel;
            Check Blocking uses
            Propagation_Line_Mathematic_Expression;
            if(Blocked)
                AddReflectionDifractionPower;
            if (ReceivedPower(i,j)>F*MaximumPower(i,j))
                P(i,j) is through;
            else
                P(i,j) is blocked;
        }
    
```


In perfect conditions, the following signal plot (Figure 22) on computer program should be revealed by the results of the measurement. Object shape can be approximated in more signal path is used in measurement.

By using signal evaluation plot as in Figure 7b, the following results are obtained by using supervised and unsupervised method. In supervised method, initial measurement is

performed before underground object inserted. Without changing the positions of transmitter and receiver, the underground object is then inserted to the center of the evaluated area. Then, both initial and final received signals are then compared.

Figure 23 plots the signal differences. The supervise method exerts 100% precise detection as the blocked signals are always lower than the unblocked signals. Average decrement is -1.86 dB.

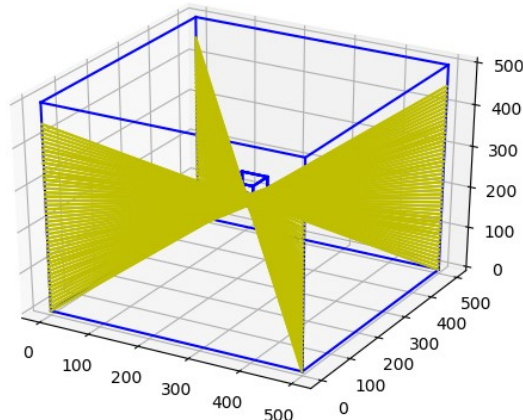


Fig.22 Signal paths that is blocked by underground object

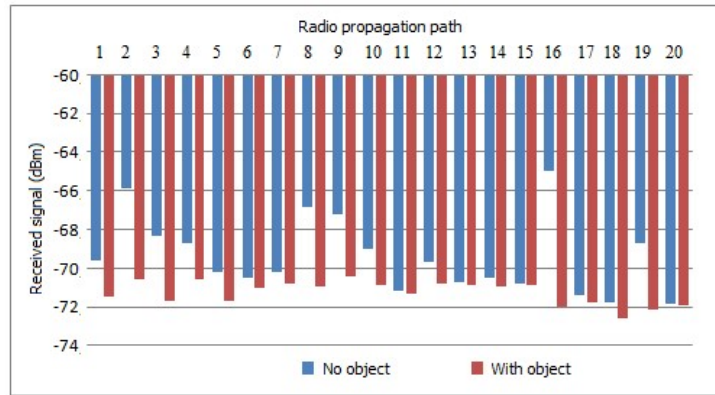


Fig.23 Supervised underground object detection

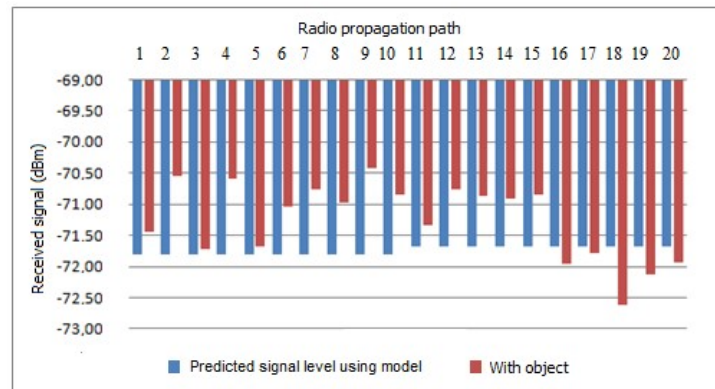


Fig.24 Unsupervised underground object detection based on Friis formula

Meanwhile, measurement by using the propagation model experience deviations as the received signals are not only coming from direct signal, but also the scattered signals and multipath signals. The blocked signals with larger distance may have higher level than the closer one.

The detection precision by using unsupervised method depends on the precision of

underground radio propagation model. As shown in Figure 24, only 30% of the predicted paths can detect the underground object. Figure 25 shows that supervised measurement exerted consistent signal decrement with average signal decrement of 1.86 dB or 2.68%. Meanwhile, only 30% signals decreased for unsupervised measurement.

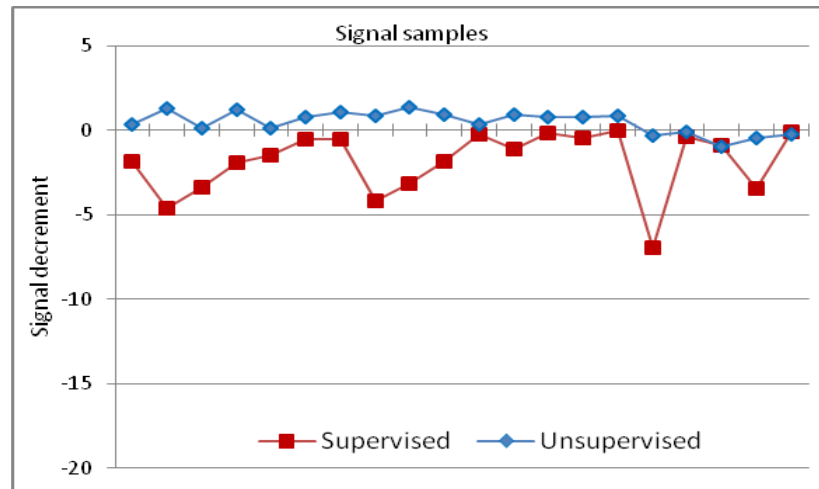


Fig.25 Supervised versus unsupervised signal decrement comparisons

5. CONCLUSIONS

This paper has analysed the use of radio propagation and received signal level to predict underground object. Radio propagation assessment has been performed by using two frequency bands: 97 MHz to 130 MHz and 500 MHz to 1 GHz. The lower frequency bands were represented by frequencies 97.335 MHz, 109.818 MHz, and 130.762 MHz, where frequency 130.762 MHz has the best precision with the smallest average model error and frequency 109.818 MHz has the best capability in detecting object with the highest signal decrement.

For frequency band 500 MHz to 1 GHz, the selected best frequency is at 537.69 MHz. By using this frequency, supervised and unsupervised measurements were performed. Supervised measurement compares the same land condition with or without object. Meanwhile, unsupervised measurement compared measurement results to propagation model. As results, supervised measurement produced better underground object detection than the unsupervised techniques. Supervised measurements obtained signal decrement due to blocking object about 1.86 dBm in average. The supervised method 100% predicted the underground object. Meanwhile, the

unsupervised measurement strongly depends on the model precision. The unsupervised method achieved only 30% prediction with signal decrement about 2.68% in average.

ACKNOWLEDGEMENT

This research has been funded by The Ministry of Research, Technology and Higher Education Republic of Indonesia (Kemenristekdikti) through Penelitian Dasar Unggulan Perguruan Tinggi (PDUPT) Schema 2019.

REFERENCES

- [1]. Minhas. U. I., Naqvi. I. H., Qaisar. S., Ali. K. Shahid. S., & Aslam. M. A. "A WSN for monitoring and event reporting in underground mine environments". IEEE Systems Journal. 12(1). 485-496, 2017.
- [2]. Dai. F., Li. B., Xu. N., Fan. Y., & Zhang. C. "Deformation forecasting and stability analysis of large-scale underground powerhouse caverns from microseismic monitoring". International Journal of Rock Mechanics and Mining Sciences. 86. 269-281, 2016.

- [3]. Yongbo W and Chen T. "Deep buried metal pipeline detection using frequency domain electromagnetic method". In AGU Fall Meeting, 2018.
- [4]. Burkes K W. Elham B M. and Ramtin H. "Water tree detection in underground cables using time domain reflectometry". IEEE Power and Energy Technology Systems Journal (2) 2 53-62, 2015.
- [5]. Liu Y H. Yunzhi H. Rui T. and Beibei W. "Application of interdigital capacitive sensors for detecting power cable insulation damage". IEEE International Conference on Mechatronics and Automation (ICMA). pp. 1795-1799, 2015.
- [6]. Ali. H.. & Choi. J. H. "A review of underground pipeline leakage and sinkhole monitoring methods based on wireless sensor networking. Sustainability". 11(15). 4007, 2019.
- [7]. Grigoli. F.. Cesca. S.. Priolo. E.. Rinaldi. A. P.. Clinton. J. F.. Stabile. T. A.. & Dahm. T. "Current challenges in monitoring. discrimination. and management of induced seismicity related to underground industrial activities: A European perspective". Reviews of Geophysics. 55(2). 310-340, 2017.
- [8]. Dahlman. O.. & Israelson. H. "Monitoring underground nuclear explosions". Elsevier, 2016.
- [9]. Salam, A. "An underground radio wave propagation prediction model for digital agriculture". Information, 10(4), p.147, 2019..
- [10]. Yoon. S. U.. Cheng. L.. Ghazanfari. E.. Pamukcu. S.. & Suleiman. M. T. "A radio propagation model for wireless underground sensor networks". In 2011 IEEE Global Telecommunications Conf. GLOBECOM, pp. 1-5, 2011
- [11]. Sun. Z.. & Akyildiz. I. F. "Channel modeling and analysis for wireless networks in underground mines and road tunnels". IEEE Transactions on communications. 58(6). 1758-1768, 2010.
- [12]. Salam, A., Vuran, M.C., Irmak, S. "Pulses in the Sand: Impulse Response Analysis of Wireless Underground Channel". In Proceedings of the 35th Annual IEEE International Conference on Computer Communications (IEEE INFOCOM 2016), San Francisco, CA, USA, 10–14 April 2016.
- [13]. Salam, A., Vuran, M.C. "Impacts of Soil Type and Moisture on the Capacity of Multi-Carrier Modulation in Internet of Underground Things". In Proceedings of the 2016 25th International Conference on Computer Communication and Networks (ICCCN), Waikoloa, HI, USA, 1–4 August 2016.
- [14]. Salam, A., Vuran, M.C. < "Irmak, S. Towards Internet of Underground Things in Smart Lighting: A Statistical Model of Wireless Underground Channel". In Proceedings of the 14th IEEE International Conference on Networking, Sensing and Control (IEEE ICNSC), Calabria, Italy, 16–18 May 2017.
- [15]. Sommerfeld, A. "Über die Ausbreitung der Wellen in der drahtlosen Telegraphie". Ann. Phys. 1909, 333, 665–736.
- [16]. Dong, X.; Vuran, M.C. "A Channel Model for Wireless Underground Sensor Networks Using Lateral Waves". In Proceedings of the 2011 IEEE Global Telecommunications Conference (GLOBECOM 2011), kathmandu, Nepal, 5–9 December 2011.
- [17]. Ian FA. "Signal propagation techniques for wireless underground communication networks". United States: Elsevier., 2009.
- [18]. C. J. Sadeghioon, A. M., Chapman, D. N., Metje, N., & Anthony, "A New Approach to Estimating the Path Loss in Underground Wireless Sensor Networks," J. Sens. Actuator Networks, vol. 6, no. 3, p. 18, 2017.
- [19]. Takahashi S, Igel K, Preetz J, Kuroda H. "Basics and application of ground-penetrating radar as a tool for monitoring irrigation process," Probl. Perspect. challenges Agric. water Manag., 2012.
- [20]. Stewart, J. "Calculus: Concepts and contexts". Cengage Learning, 2009.